



HAL
open science

Bisoxazolidine vs Imine ligands and Zn-complexes formation: experimental and theoretical calculations

Paola Sánchez-Portillo, David Morales-Morales, Jean M Grévy, Pascal G. Lacroix, Victoria Elena González Flores, Victor Barba

► To cite this version:

Paola Sánchez-Portillo, David Morales-Morales, Jean M Grévy, Pascal G. Lacroix, Victoria Elena González Flores, et al.. Bisoxazolidine vs Imine ligands and Zn-complexes formation: experimental and theoretical calculations. Journal of Molecular Structure, 2024, 1310, pp.138306. 10.1016/j.molstruc.2024.138306 . hal-04590913

HAL Id: hal-04590913

<https://hal.science/hal-04590913v1>

Submitted on 28 May 2024

HAL is a multi-disciplinary open access archive for the deposit and dissemination of scientific research documents, whether they are published or not. The documents may come from teaching and research institutions in France or abroad, or from public or private research centers.

L'archive ouverte pluridisciplinaire **HAL**, est destinée au dépôt et à la diffusion de documents scientifiques de niveau recherche, publiés ou non, émanant des établissements d'enseignement et de recherche français ou étrangers, des laboratoires publics ou privés.

Bisoxazolidine vs Imine ligands and Zn-complexes formation: experimental and theoretical calculations

Paola Sánchez-Portillo,¹ David Morales-Morales,² Jean M. Grévy,¹ Pascal G. Lacroix,³ Victoria Elena González Flores¹ and Victor Barba^{1*}

¹*Centro de Investigaciones Químicas-IICBA, Universidad Autónoma del Estado de Morelos Av. Universidad 1001, C.P. 62209 Cuernavaca, Morelos México.*

²*Instituto de Química, Universidad Nacional Autónoma de México, Circuito Exterior S/N, Ciudad Universitaria, C.P. 04510 Coyoacán, México City. México.*

³*CNRS, LCC (Laboratoire de Chimie de Coordination), 205, Route de Narbonne, F-31077 Toulouse, France.*

*Corresponding Author: E-mail addresses: vbarba@uaem.mx (V. Barba)

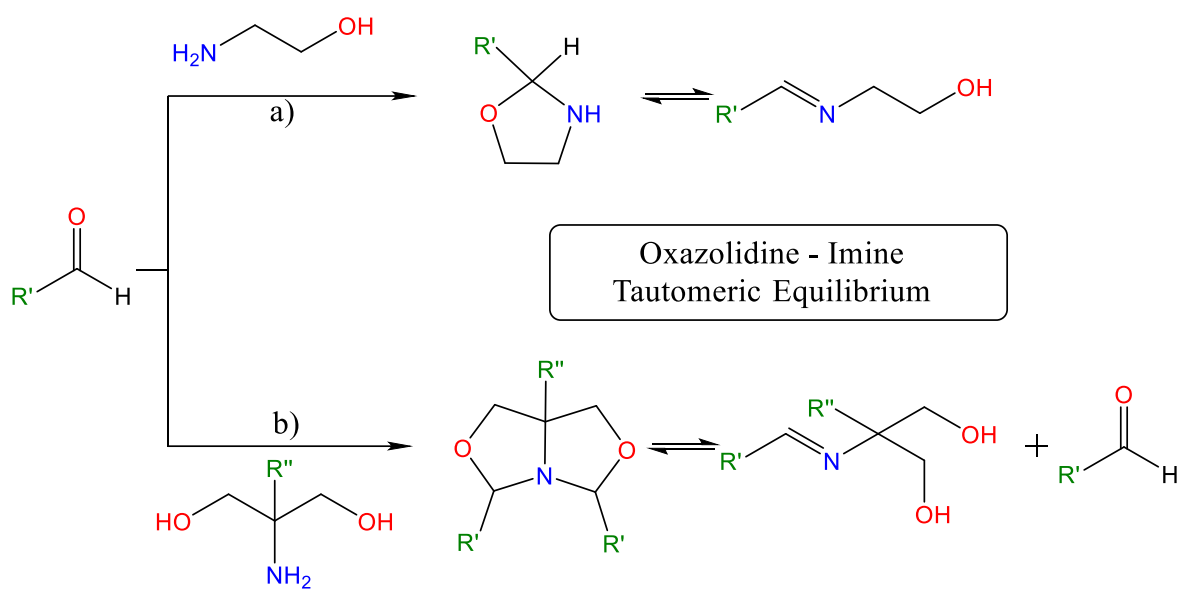
Abstract

The condensation reaction between aminodiols and carboxaldehydes offers the possibility to obtain either bisoxazolidine or imine compounds. However, limited information is available regarding the factors influencing this behavior. Thus, the present work investigates the substituent effect on the reactivity of aminodiols with pyridine carboxaldehydes both in the presence and absence of Zn (II). Without the presence of the metal, the condensation reactions favor the production of bisoxazolidine derivatives, with identification of both *cis* and *trans* isomers in relation to the pyridyl moieties. Notably, the presence of a methyl substituent favors the *trans* isomers owing to the steric hindrance effect, while a hydrogen substituent favors the *cis* isomers. Conversely, in the presence of ZnCl₂, the main product is the imine-metal complex when the substituent is a methyl group. However, in the presence of a hydrogen substituent, both the imine-metal and the bisoxazolidine-metal complexes were produced as a mixture in similar proportions. These experimental results are supported by theoretical calculations.

Keywords: Oxazolidines, imine, zinc complex, tautomeric equilibrium, isomers

1. Introduction

Oxazolidines are heterocyclic compounds formed through the straightforward condensation between aldehydes and amino-alcohols (Scheme 1a). These compounds have garnered significant attention for numerous applications including the formation of chiral compounds [1-3], catalysis [4-7] and medicinal purposes [8, 9]. The dynamic nature of oxazolidines involves a tautomeric equilibrium with imine/alcohol compounds (Scheme 1) [10-13], influenced by various factors such as solvent, temperature, and nature of the substituents present in the starting materials [14, 15].



Scheme 1. Oxazolidine (a) and bisoxazolidine (b) formation and their tautomeric equilibrium with imine like derivatives.

Besides, the presence of both nitrogen and oxygen atoms in the oxazolidine structures enables these species to use it as coordinating ligands for different metal centers; indeed, numerous coordination metal complexes including cobalt, copper, cadmium, iron, palladium, nickel, manganese, zinc and mercury have been described [16-25]. Notably, the presence of pyridyl moieties in the structure, has been showed to favor the formation of the oxazolidine-metal complexes over the imine-metal compounds [26, 27]. In fact, Oliveira *et al.* described a potential mechanism involved in the conversion imine to oxazolidine-like compounds in a

series of copper derivatives [21]. On the other hand, Mayans *et al.* provided structural evidence for the coexistence of imine and oxazolidine-like compounds using nickel and manganese metal centers [20]. Similarly, in the context of palladium as the metal center, Molaee *et al.* observed the simultaneous formation of oxazolidine-metal and imine-metal complexes. Their findings established a direct correlation between the nature of the substituent and the structure of complexes formed. Precisely, the only presence of a methyl group at specific position favored the oxazolidine-metal complex, while the imine-metal complex was favored in the presence of a hydrogen atom as substituent [19]. Building in this, a more recent work by Mardani reported that using copper or cadmium as metal centers in the reaction of an amino alcohol with the corresponding aldehyde led to a mixture of oxazolidine/imine metal complexes [28].

It is noteworthy that when employing aminodiols as reagents (Scheme 1b), bisoxazolidine-like compounds are obtained [29], a category of compounds less studied than its mono-oxazolidines counterpart. Thus, the equilibrium between imine and bisoxazolidine has been less studied so far. Previous research in this field was focused on the stereochemistry of isomers, the conformation of the fused cycles and the anomeric effect [29]. Remarkably, there are only few examples of bisoxazolidines coordinated to metal centers. Recently, Jones *et al.* explored the use of a bisoxazolidine functionalized with pyridyl motifs forming complexes with metal(II) ions including manganese, iron, cobalt, manganese and copper. Their findings highlighted the correlation between the ligand's structural configuration and the steric effect of the substituents, influencing the binding mode [30]. Furthermore, the authors investigated the application of bisoxazolidine iron complexes as catalysts for a dehydration processes, showing selective conversion of 1-phenyl-ethanol to styrene with high yields [31]. A similar iron complex reported by Das was obtained from tris(hydroxymethyl) aminomethane and 2-pyridine carbaldehyde with iron (II) chloride, the referred compound demonstrated its utility as a catalyst for the oxygen production. The bisoxazolidine-metal complex produced, allows the formation of O-O bonds, this being the crucial step for water oxidation reactions [32].

In this context, we investigated the reactivity of aminodiols with pyridine carboxaldehydes. Initially, reactions were conducted in the absence of metal, followed by subsequent reactions in the presence of Zn (II). In metal free conditions, reactions mainly led to the bisoxazolidine compounds affording two isomers (*cis/trans*) regarding to the pyridine moieties. On the other hand, the introduction of Zn (II) enables the formation of both oxazolidine and imine tautomeric forms as their corresponding metal complexes. In addition, the effect of the aminodiol substituents on the formation of either bisoxazolidine or imine derivative was analyzed. The experimental findings are supported by DFT computational analyses.

2. Results and discussion

2.1 Reactivity of aminodiols with pyridine carboxaldehydes

The direct condensation reaction between 2-amino-1,3-propanediols and pyridine carboxaldehydes produces bisoxazolidine-like products with *cis* or *trans* configurations. To investigate the impact of the aminodiol substituents (using -H and -CH₃) and the substitutions achieved on the pyridine carboxaldehyde derivative (2-pyridinecarboxaldehyde, 3-pyridinecarboxaldehyde and 4-pyridine carboxaldehyde) on the isomeric distribution of the final products, reactions were conducted as outline in Scheme 2. The reactions were performed in a heating reactor *Monowave50* under pressure at 130°C for 30 minutes using a methanol/toluene solvent mixture (1:1, v/v). Compounds **1a** and **1c** were obtained as white solids, while compounds **1b** and **1d** were obtained as yellow oils. All four products were obtained in moderate to high yields and exhibited high solubility in common organic solvents such as chloroform and methanol.

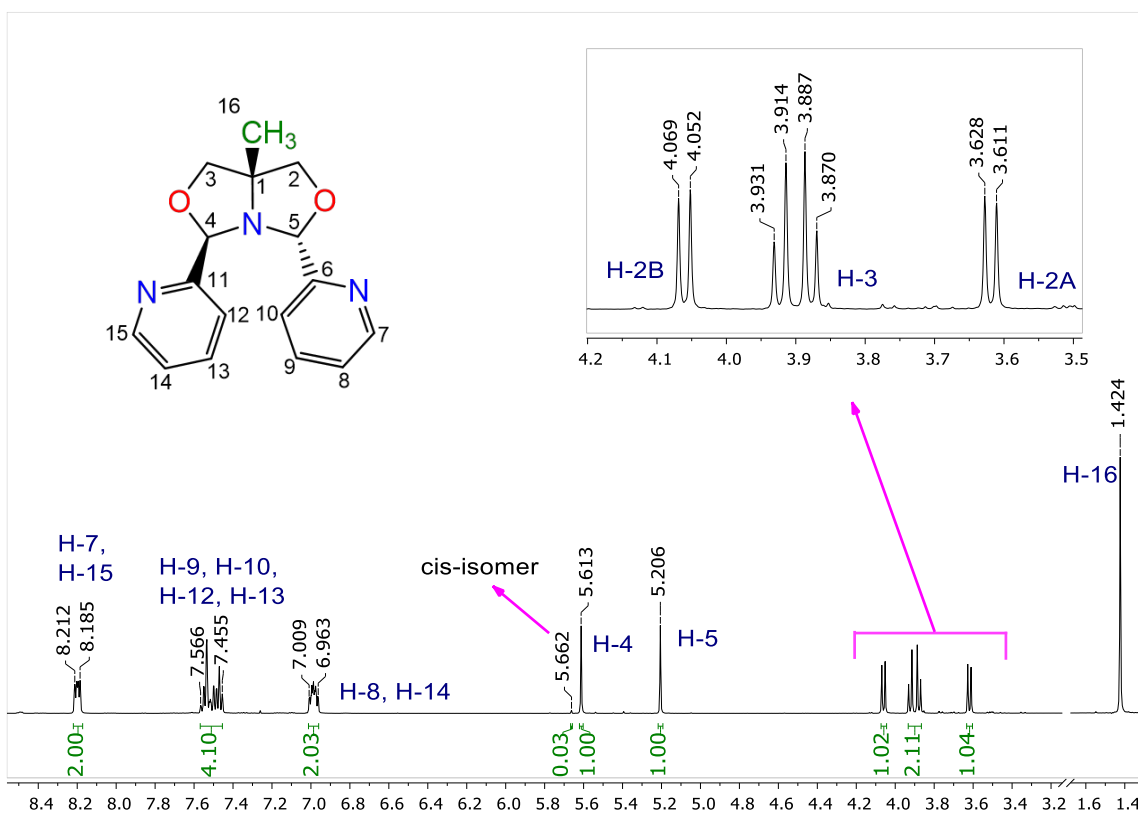
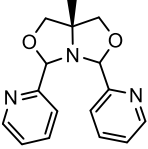
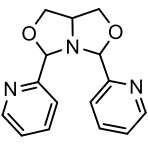
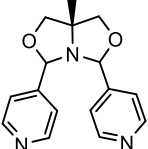
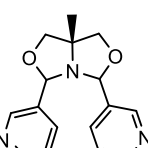


Figure 1. ^1H NMR spectra of compound **1a** as *trans/cis* isomer mixture in CDCl_3 (500 MHz).

Additionally, when serinol served as the aminodiol precursor, compound **1b** was obtained as a yellow oil in 86 % yield. This oil was analyzed by ^1H NMR spectroscopy, revealing also the presence of both *cis* and *trans* isomers, but with the *cis* isomer emerging as the major product (85:15 ratio, Table 1, Fig. S2). The *cis* isomer displayed a single signal for the hydrogen atoms of the CH groups H4, H5 at $\delta = 5.71$ ppm [34]. These findings emphasize the significance of the aminodiol substituent (H or Me) on dictating the formation of either the *cis* or *trans* isomers. As noticed above, employing methyl as the substituent favors the *trans* isomer, while using hydrogen as the substituent predominantly yielded the *cis*-isomer.

Table 1. Yield and *trans* : *cis* ratio of the bisoxazolidine products

Label	Product	Yield [%] ^[a]	<i>trans</i> : <i>cis</i> ^[b] ratio
-------	---------	--------------------------	--

1a		89	97:3
1b		86	15:85
1c		90	94:6
1d		90	ND ^[c]

[a] Yield of the isolated product. [b] Determined “in situ” by ¹H NMR. [c] Not Determinate

From the condensation reaction involving 4-pyridinecarboxaldehyde and 2-amine-2-methyl-1,2-propanediol, a white solid was obtained in 90 % yield (**1c**). ¹H NMR spectra revealed the formation of the bisoxazolidine including the presence of the *trans/cis* isomers mixture, with the *trans*-isomer as the major product in a 94:6 ratio. Notably, the characteristic signals for the hydrogens 4 and 5 were observed at $\delta = 5.52$ and 5.05 ppm, respectively, corresponding to the *trans* isomer (Fig. S3). This observation highlights the influential role of the methyl group in the preference for the *trans* isomer.

On the other hand, the reaction between 3-pyridinecarboxaldehyde and 2-amine-2-methyl-1,3-propanediol yielded a yellow oil. The ¹H NMR analysis of this compound indicates the presence of multiple signals, signifying the formation of various byproducts that proved challenging to separate/isolate using standard procedures. Drawing inspiration from previous work employing Lewis acids as catalyst for the preparation of similar compounds [35], the reaction was conducted in the presence of 1,4-benzen diboronic acid as catalyst. Using similar conditions to those used for the synthesis of **1a**, a yellow oil was obtained. Although the ¹H NMR analysis of this oil revealed a complex mixture of products difficult to isolate, it was possible to identify the characteristic set of signals for H4 and H5 assigned to the *trans*-isomer at $\delta = 5.46$ and $\delta = 5.06$ ppm, as those observed for compound **1a**. Fortunately, a

single crystal suitable for X-ray diffraction analysis was obtained. The resulting structure confirmed the formation of the *trans* bisoxazolidine (**1d**) and notably, the unit cell showed the inclusion of a molecule of the Lewis acid catalysts 1,4-benzene diboronic acid (Figure 2). The bisoxazolidine structure exhibits a distorted envelope-type conformation for the two 5-membered heterocycles, with the nitrogen N(2) and carbon C(14) atoms forming the border of the house-roof conformation and the two oxygen atoms (O5 and O6) located at the tip of the envelope conformation. This conformational behavior observed in analogous derivatives, has been attributed to the anomeric effect [34]. Furthermore, the pyridyl substituents are found in opposite sides of the envelope, one in the equatorial position and the other in the axial position, thus confirming the *trans*-isomer, as indicated by the ¹H NMR results.

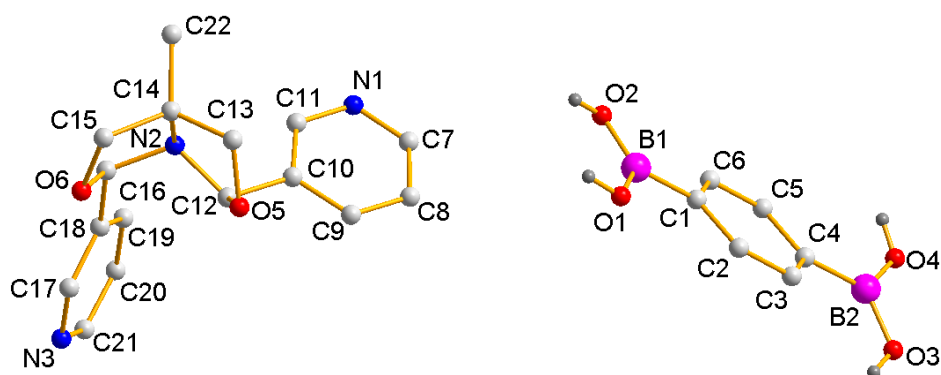


Figure 2. Molecular structure of the *trans*-isomer (**1d**). Selected distances (Å) and angles (°): N(2)-C(16): 1.4608 (19), N(2)-C(12): 1.4704 (19), C(16)-O(6): 1.4226 (18), O(6)-C(15): 1.4300 (19), C(15)-C(14): 1.552 (2), C(14)-C(13): 1.530 (2), C(14)-N(2): 1.4986 (19), C(13)-O(5): 1.4352 (18), O(5)-C(12): 1.4328 (18). C(16)-N(2)-C(12): 115.51 (12), O(5)-C(13)-C(14): 104.03 (12), C(15)-O(6)-C(16): 103.24 (11), C(16)-N(2)-C(14): 103.64 (11).

In the solid state, the connection among bisoxazolidine and the diboronic acid is evident through hydrogen bond interactions, specifically between the hydroxyl groups of the diboronic acid and the nitrogen atoms of the pyridine moiety forming O-H \cdots N interactions (1.914 Å). Additionally, two O-H \cdots O interactions involving the hydroxyl of the boronic groups with hydrogen bond distances of 1.912 and 1.8896 Å, link two boronic acid fragments forming 2D polymeric chains (Figure 3).

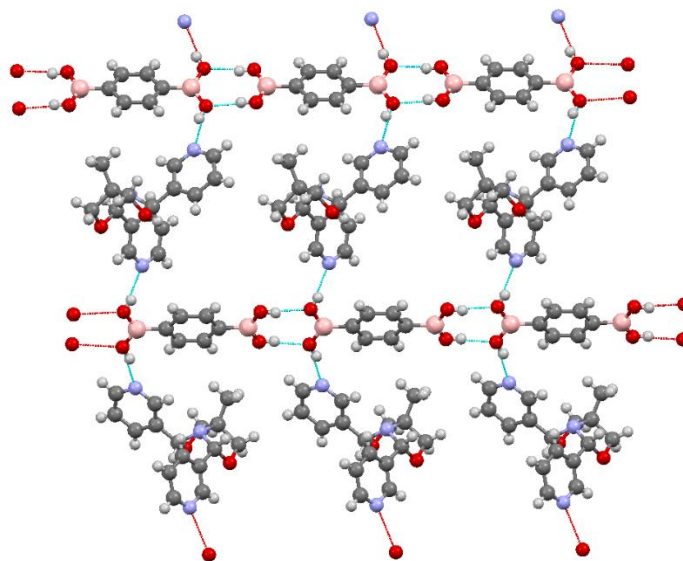


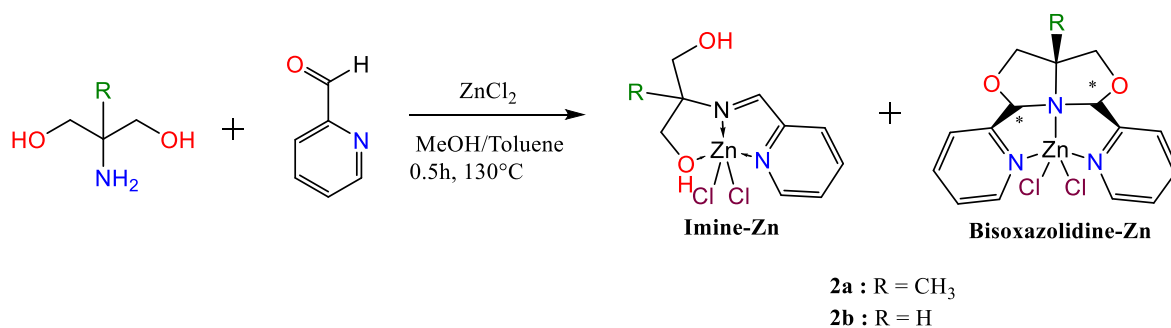
Figure 3. 2D polymeric sheet supported by O-H...N and O-H...O interactions.

All four compounds were characterized by mass spectrometry, revealing the presence of the molecular ions detected at $m/z = 283$ for **1a**, **1c** and **1d**, and $m/z = 270$ for **1b**. These data provide additional evidence supporting the formation of bisoxazolidines. Remarkably, it is important to emphasize that in no case the imine like compound was detected.

2.2 Reactivity of aminodiols with pyridine carboxaldehydes in the presence of $ZnCl_2$

As mentioned above, the reaction of pyridylcarboxaldehydes with aminodiols in the presence of metal salts can lead to the formation of imine derivatives, nonetheless, it is known that coordination compounds including bisoxazolidines-like compounds, can also be obtained in such reactions [30,31].

To explore the potential formation of imine or bisoxazolidine compound, the condensation reaction of aminodiols and 2-pyridinecarboxaldehyde was conducted in the presence of $ZnCl_2$. All reagents were dissolved in a methanol/toluene solvent mixture (20:80) and the resulting reaction mixture heated for 30 min at $130^\circ C$ using a *Monowave 50* heating reactor (Scheme 3).



Scheme 3. Reactivity between aminodiols and 2-pyridinecarboxaldehyde in the presence of ZnCl₂.

The reaction using 2-amino-2-methyl-1,3-propanediol as the starting material led to the compound **2a** as a white solid in 87 % yield. IR spectroscopy analysis revealed a well-defined band at $\nu = 1660 \text{ cm}^{-1}$, matching for the presence of the imine group (C=N_{imine}) as previously reported for similar complexes [36].

Further characterization by ¹H NMR spectroscopy (Fig. S4) provided evidence for the imine complex being the compound namely as **2a-imine** the only isolate product. The characteristic signal for the hydrogen atom of the imine moiety (H-6) appeared at $\delta = 8.83 \text{ ppm}$, and signals for the aromatic hydrogens were observed in the usual region between $\delta = 8.60$ and 7.83 ppm . In addition, only one AB system can be observed at high field, corresponding to the 4 hydrogens of the 2 methylene fragments (CH₂-8, CH₂-10), thus suggesting a rapid interchange between both CH₂OH groups in solution. The chemical shifts appear like those observed in related compounds previously reported [36, 37].

Suitable crystals for single crystal X-ray diffraction analysis were obtained by slow evaporation of a concentrated methanol solution, thus unequivocally confirm the molecular structure of compound **2a-imine** (Figure 4). The structure revealed two fused five-membered chelate rings forming an heterobicycle with a N→Zn coordination bond.

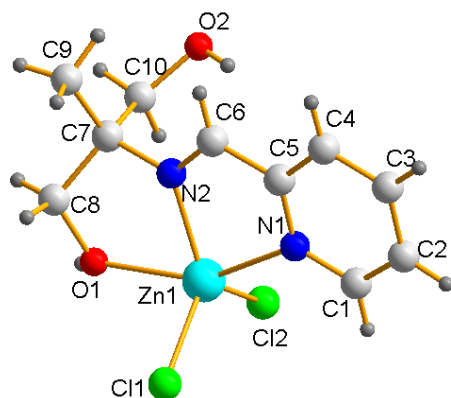


Figure 4. Molecular structure of compound **2a-imine** obtained by X-ray diffraction.

The molecular structure reveals a Zn atom in a pentacoordinate environment, establishing three coordination bonds with the ligand: one with the nitrogen atom of the pyridyl group (N_{py}), another with the nitrogen atom of the imine group (N_{imine}), and a third with the oxygen atom of one hydroxyl group. Two chloride atoms complete the coordination sphere of the metal center. Remarkably, the Zn- N_{imine} distance [2.208(5) Å] is shorter than the Zn- N_{py} distance [2.249(4) Å] (Table 2), a behavior already observed for analogous complexes [38, 39].

Pentacoordinate systems typically can adopt any distorted geometry from square pyramidal to trigonal bipyramidal geometries. Thus, to discern the geometry, the τ value was calculated using the equation $\tau = (\beta - \alpha) / 60$, where β and α are the larger angles around the central atom. For an ideal square pyramidal geometry, $\tau = 0$ and the angles $\beta = \alpha = 90^\circ$, whereas for an ideal trigonal bipyramidal geometry, $\tau = 1$ and $\alpha = 120^\circ$ [40]. In our present case, compound **2a-imine** exhibits values of $\tau = 0.51$ and $\alpha = 122.6^\circ$ corresponding to a distorted trigonal bipyramidal geometry with the two chloride and the iminic nitrogen atoms located at equatorial positions, while the nitrogen atom of the pyridine moiety and the oxygen atom of the hydroxyl moiety are located in axial positions.

Table 2. Selected bond distances (Å) and angles (°) for compounds **2a-imine**, **2b-imine**, **2b-bisoxazolidine**.

	2a-imine	2b-imine	2b-bisoxazolidine
Zn(1)-O(1)	2.249(4)	2.312(2)	
Zn(1)-N(1)	2.208(5)	2.152(2)	2.3441(12)
Zn(1)-N(2)	2.064(5)	2.073(2)	2.1016(13)
Zn(1)-Cl(1)	2.266(2)	2.2659(8)	2.3404(4)
Zn(1)-Cl(2)	2.251(2)	2.2302(8)	2.2670(4)
Zn(1)-N(3)	--	--	2.0893(13)
N(1)-Zn(1)-O(1)	153.2(2)	152.84(8)	
N(2)-Zn(1)-Cl(2)	122.6(2)	122.76(7)	
Cl(2)-Zn(1)-Cl(1)	115.92(7)	115.63(3)	105.062(14)
Cl(1)-Zn(1)-N(2)	120.8(2)	120.35(7)	
Cl(2)-Zn(1)-N(1)			99.57(3)
N(3)-Zn(1)-Cl(1)			96.21(3)
N(3)-Zn(1)-N(1)			76.08(5)
N(2)-Zn(1)-N(1)			76.65(5)
N(3)-Zn(1)-Cl(2)			111.29(4)
N(3)-Zn(1)-N(2)			138.20(5)

In solid state, only one hydroxyl group coordinates with the zinc atom, forming a 5-member chelate, while the other OH group remains uncoordinated. This contrast with the observation of only one set of signals by NMR corresponding to the methylene groups (CH₂OH) in solution. Consequently, these results suggest a rapid equilibrium in solution between the two hydroxyl groups, alternating between coordinate and uncoordinated states to the metal center.

Furthermore, the reaction between 2-pyridincarboxaldehyde and 2-amino-1,3-propanediol in the presence of ZnCl₂, under similar conditions to those used for compound **2a**, produced a white solid in 45% yield. The ¹H NMR analysis revealed the presence of two distinct sets of signals, corresponding to the imine (**2b-imine**) and the other to the bisoxazolidine derivative (**2b-bisoxazolidine**), approximately in a 1:1 ratio. For the imine derivative, the characteristic signal for the HC=N fragment was observed at δ = 8.03 ppm, moreover, a single broad signal

at $\delta = 5.15$ ppm assigned to the OH group indicating the coordination to the metal center, mirroring the behavior observed for compound **2a**. Additionally, the single signal at $\delta = 6.35$ ppm was assigned to the hydrogen of the CH groups of the bis-oxazolidine derivative (Figure S5). Suitable crystals for single crystal X-ray diffraction analysis were obtained by slow evaporation of a saturate ethanol solution, from which two different crystals were grown, separate and collected allowing the unequivocal determination of the structures of both the **2b-imine** and the **2b-bisoxazolidine** compounds (Figure 5).

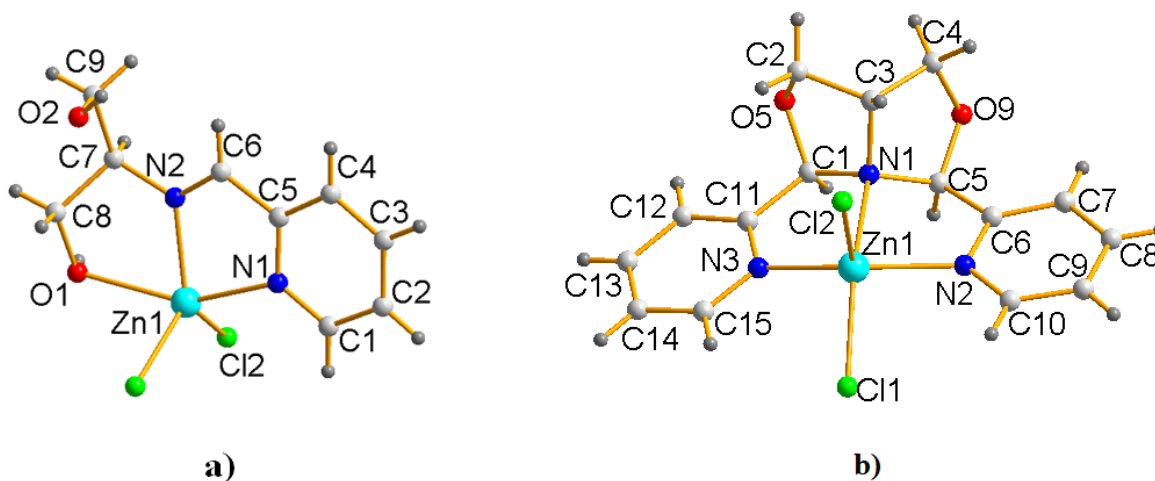


Figure 5. Molecular structures obtained for **2b-imine** (a) and **2b-bisoxazolidine** (b) compounds determined by X-ray diffraction analysis.

The molecular structure of **2b-imine** exhibited similar bond distances and angles as those observed for **2a-imine**. The values of $\tau = 0.50$ and $\alpha = 122.7^\circ$ also indicated the same distorted trigonal bipyramidal zinc geometry, some differences were found though, for instance the Zn(1)-O(1) bond distance is slightly longer than that found in **2b-imine** (2.323(2) Å), while the Zn(1)-N(1) bond distance is shorter [2.152(2) Å] (Table 2). Thus, allowing to conclude that for imine complexes (**2a**, **2b**) not noticeable effect related to the presence of different substituents (hydrogen or methyl) can be observed.

Besides, for both compounds (**2a-imine** and **2b-imine**), non-covalent hydrogen bonding interactions (C-H \cdots O, C-H \cdots Cl, O-H \cdots O and O-H \cdots Cl) were observed in the solid state (Table 3). For instance, compound **2a-imine** showed O-H \cdots Cl and O-H \cdots O hydrogen bonds with distances of 2.348 and 1.914 Å, respectively. These interactions result in the formation of

tetrameric arrangements and in turn, supramolecular cycles of 20 members $R_4^4(20)$ are observed (Figure 6a). In addition, in compound **2b-imine** C-H \cdots Cl and C-H \cdots O hydrogen bonds are observable with distances of 2.843 and 2.529 Å, respectively, forming 26-member supramolecular cycles $R_4^4(26)$ (Figure 6b).

Table 3. Hydrogen bonds in compounds **2a-imine** and **2b-imine**.

Compound	Interaction	Distance (Å)	Distance (Å)	Angle (°)	Symmetry codes
		D-H \cdots A	H \cdots A	D-H \cdots A	
2a-imine	O(2)-H(2A) \cdots Cl(1)	3.092	2.348	175.33	-1+x,y,z
	O(1)-H(1A) \cdots O(2)	2.691	1.914	164.58	-1/2x,1/2-y,1/2z
	C(2)-H(2) \cdots Cl(2)	3.562	2.843	135.01	-1/2+x,-1/2-y,1-z
2b-imine	O(1)-H(1A) \cdots Cl(1)	3.103	2.261	165.49	-1/2+x,1/2-y,1-z
	C(9)-H(9C) \cdots O(2)	3.463	2.529	164.48	1-x,1/2+y,1/2-z

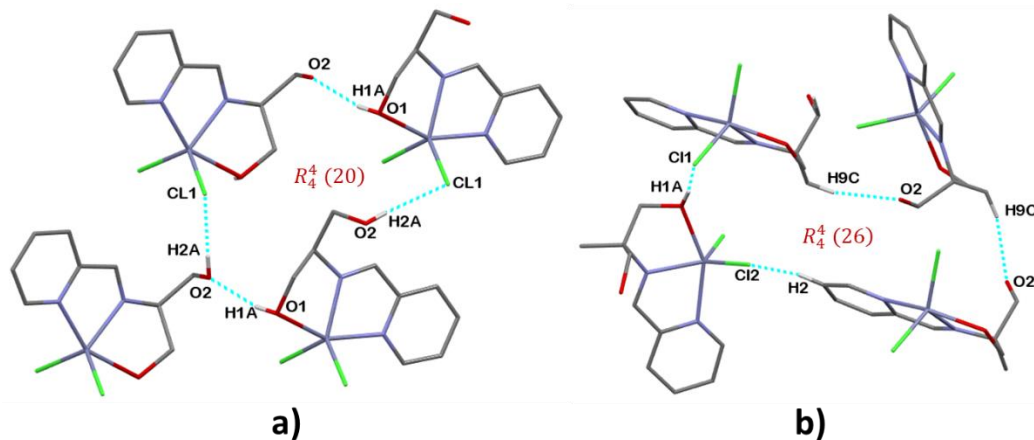


Figure 6. Supramolecular arrangements formed by C-H \cdots Cl, C-H \cdots O, O-H \cdots Cl and O-H \cdots O no-covalent interactions for compounds **2a-imine** and **2b-imine**.

On the other hand, the structural analysis of compound **2b-bisoxazolidine** showed the zinc center to be also pentacoordinate, forming four fused five-membered heterocycles in the central part (Figure 5b). Three nitrogen atoms and two chlorines atoms around the metal center constitute the five-coordination geometry. The Zn-N_{py} distances are shorter [2.0891(13) and 2.1016(13) Å] than the Zn-N_{aliph} distance of the aliphatic nitrogen atom [2.3441(12) Å], this being attributable to the fact that the pyridine nitrogen atom has a sp^2

hybridization, a behavior previously observed in analogous systems [41]. It is important to remark that the two pyridyl moieties are in a *cis* arrangement with respect to each other. The pentacoordinate zinc atom is closer to a square-based pyramid geometry, as indicated by the angles around the zinc atom with α values ranging from 75.65(5) to 99.57(3) $^\circ$ and a τ value of 0.28. The three nitrogen atoms and one chloride atom are situated at the basal positions, while the additional chloride atom is located at the apical position of the pyramidal arrangement.

3. Theoretical calculations

The experimental findings revealed the influence for the product formation of the substituent R (H or Me) present in the aminoalcohol. The bisoxazolidine-like compounds consist on two fused five-membered heterocycles adopting a house-roof conformation, leading to different orientations between the -R substituent and the pyridyl groups. The *cis* isomer is favored when R = H, orienting the two pyridine groups towards the same side. Conversely, when R = Me, the *trans* conformation is favored, with the two pyridyl groups oriented in opposite sides due to steric hindrance effect of the methyl group (Scheme 2). To support these observations, the *cis* and *trans* bisoxazolidine isomers were fully optimized using the Gaussian-09 program package [42] within the framework of the Density Functional Theory (DFT), (Figure 7). The combination of the widely used B3LYP hybrid functional [43,44], with the double- ζ basis set 6-31G** [45], was employed in which polarization functions are introduced to account for potential hydrogen bonding. A potential equilibrium was suggested (Scheme 4) for the presence of both isomers. The Gibbs free energies (G) were calculated for the *cis-trans* isomers for which $\Delta G = G_{trans} - G_{cis}$. Considering both substituents (R= H, Me), the observed values were $\Delta G = 1.56 \text{ kcal mol}^{-1}$ for R = H and $-1.07 \text{ kcal mol}^{-1}$ for R = CH₃. The trend indicates that the *trans*-isomer becomes favored when R = CH₃, due to the appearance of an additional methyl...pyridine steric hindrance in the *cis*-isomer, therefore, the preference for the *cis*-isomer observed experimentally when R = H is supported by the computational data.

Besides, the calculated bond distances and angles for all *cis/trans* isomers are very related to those values observed experimentally for compound **1d**. However, some important differences were identified in the torsion angles N(3)-C(11)-C(10)-N(2) and N(1)-C(5)-C(6)-N(2) for the **1a-cis** isomer, which exhibited lower values compared to the same angles in the **1b-cis** isomer. This observation could be attributed to an increase in the steric restrictions and correlated with the no experimental isolation of this isomer (Table 4).

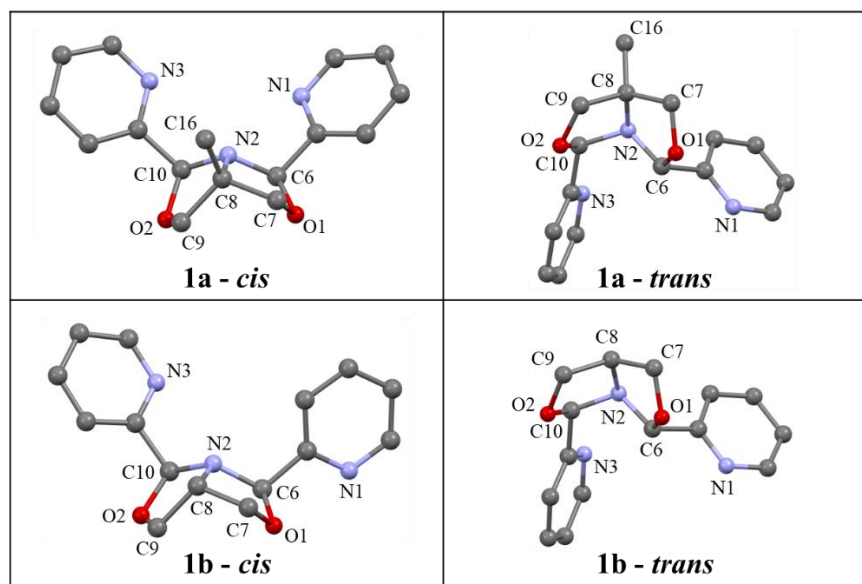


Figure 7. Optimized molecules geometries for bisoxazolidines *cis/trans* isomers.

Table 4. Selected distances, angles and torsion angles optimized for bisoxazolidine molecules, *cis* and *trans* isomers.

	Distances (Å)			
	<i>1a-cis</i>	<i>1a-trans</i>	<i>1b-cis</i>	<i>1b-trans</i>
N(2)-C(6)	1.484	1.476	1.450	1.478
C(6)-O(1)	1.422	1.435	1.437	1.434
O(1)-C(7)	1.428	1.425	1.429	1.427
C(7)-C(8)	1.535	1.533	1.543	1.526
C(8)-C(9)	1.564	1.570	1.538	1.561
C(9)-O(2)	1.432	1.430	1.429	1.431

O(2)-C(10)	1.432	1.428	1.410	1.428
C(10)-N(2)	1.456	1.464	1.491	1.465
N(2)-C(8)	1.493	1.495	1.492	1.486
Angles (°)				
N(2)-C(6)-O(1)	107.28	107.07	106.61	107.00
O(1)-C(7)-C(8)	104.35	103.94	103.19	103.23
C(8)-C(9)-O(2)	106.55	106.36	105.92	105.79
O(2)-C(10)-N(2)	106.73	106.20	107.66	106.29
C(10)-N(2)-C(8)	105.63	103.60	105.83	103.39
C(6)-N(2)-C(8)	106.68	106.68	106.96	106.27
Torsion Angles (°)				
C(11)-C(10)-N(2)-C(8)	90.92	-162.04	95.90	-160.90
C(5)-C(6)-N(2)-C(8)	-116.96	-116.15	-119.60	-117.47
N(3)-C(11)-C(10)-N(2)	57.93	-67.41	71.23	-67.43
N(1)-C(5)-C(6)-N(2)	-60.58	-172.18	-167.19	-168.87

Furthermore, computational studies for the bisoxazolidine-Zn complexes namely **2a-bisoxazolidine** and **2b-bisoxazolidine** were conducted (Figure 8, Table 5). X-ray diffraction analysis indicated that a *cis* disposition of the pyridyl groups favors the formation of the bisoxazolidine-Zn complexes, being this conformation unfavorable for the methyl derivative owing steric repulsions. Calculations also revealed that the *cis* conformation is stabilized *versus* the *trans* isomer, in full agreement with the experimental findings. The Gibbs energy difference between the *cis* and *trans* isomers were calculated to be 4.20 kcal mol⁻¹ when R = H and 4.56 ~~2.55~~ kcal mol⁻¹ for R-CH₃, with the *cis* conformation being favorable. The potential transformation from bisoxazolidine-Zn to the imine-Zn was considered through a hydrolysis reaction as depicted in the following reaction:



Calculations revealed that the imine-Zn complex is only slightly favored for the hydrogen derivative with $\Delta G = -0.91$ ~~-0.59~~ kcal mol⁻¹, in comparison with the higher value observed

for the methyl derivative ($\Delta G = -0.51$ -2.26 kcal mol⁻¹). These results align well with the experimental data, indicating that both bisoxazolidine-Zn and imine-Zn complexes are observed, almost in equal proportions, when R = H, while the Imine-Zn species is dominant when R = CH₃.

The structural analysis conducted through calculations for imine and bisoxazolidine like derivatives (Figure 8, Table 5) showed a close agreement between the experimental data obtained from X-ray diffraction analysis and the computed bond distances and angles.

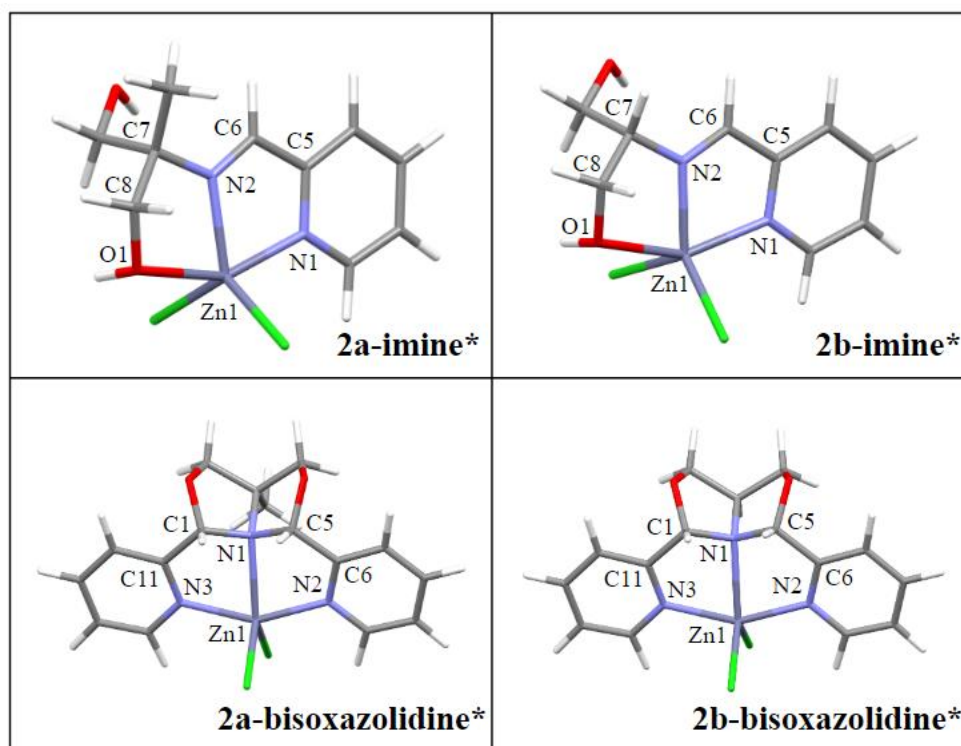


Figure 8. Optimized molecules geometries for bis-oxazolidine-Zn and imine-Zn complexes.

Table 5. Selected distances and angles of optimized molecules geometries for bisoxazolidine-imine zinc complexes

	Distances (Å)			
	<i>2a-imine*</i>	<i>2b-imine*</i>	<i>2a-bisoxazolidine*</i>	<i>2b-bisoxazolidine*</i>
Zn(1)-N(1)	2.160	2.168	2.378	2.368
Zn(1)-N(2)	2.095	2.080	2.087	2.088
Zn(1)-O(1)	2.281	2.346	N/A	N/A

Zn(1)-N(3)	N/A	N/A	2.087	2.90
Angles (°)				
Zn(1)-N(1)-C(5)	112.45	112.37	N/A	N/A
C(5)-C(6)-N(2)	118.71	118.41	N/A	N/A
N(2)-C(7)-C(8)	106.03	107.53	N/A	N/A
C(8)-O(1)-Zn(1)	110.63	110.10	N/A	N/A
O(1)-Zn(1)-N(2)	75.15	74.43	N/A	N/A
N(1)-Zn(1)-N(2)	77.74	77.52	N/A	N/A
Zn(1)-N(2)-C(6)	N/A	N/A	119.17	120.23
C(6)-C(5)-N(1)	N/A	N/A	110.68	110.84
N(1)-C(1)-C(11)	N/A	N/A	110.65	110.55
C(11)-N(3)-Zn(1)	N/A	N/A	119.11	119.66
N(3)-Zn(1)-N(1)	N/A	N/A	75.42	75.25
N(2)-Zn(1)-N(1)	N/A	N/A	75.43	75.45

N/A = Not applicable

3. Experimental

3.1. Materials and measurements

All reagents and solvents were acquired from commercial suppliers and used without further purification. The ^1H and ^{13}C spectra were recorded at room temperature using a Varian Mercury 200 MHz and Bruker Avance 500 MHz spectrometers and CDCl_3 and DMSO-d_6 as solvents. TMS (internal, ^1H , $\delta = 0.00$ ppm, ^{13}C , $\delta = 0.0$ ppm) was used as standard reference. Mass spectra were obtained with Jeol JMS 700 equipment. Melting points were determined with a Büchi B-540 digital apparatus. Crystal intensity data were collected at $T = 100$ K using Cu-K α radiation $\lambda = 1.54184$ Å, for **1d** and **2b-bisoxazolidine** (Mo-K α radiation $\lambda = 0.71073$ Å for **2a-imine** and **2b-imine**), graphite monochromator on an Agilent Technologies SuperNova diffractometer equipped with the EOsS2 CCD area detector and an Oxford Instruments Cryogen cooler. Crystal data, data collection parameters and convergence results are listed in Table S1. The measured intensities were reduced to F^2 and corrected for absorption using spherical harmonics (CryAlisPro) [46]. Intensities were corrected for Lorentz and polarization effects. Structure solution, refinement, and data output

were performed with the OLEX2 program package [47] using SHELXL-2014 [48] for the refinement. Non-hydrogen atoms were refined anisotropically. All hydrogen atoms were placed in geometrically calculated positions using the riding model. Intermolecular distances were analyzed with MERCURY [49] and DIAMOND [50]. CCDC Nos. 2286409 (**1d**), 2286410 (**2a-imine**), 2286413 (**2b-imine**) and 2286414 (**2b-bisoxazolidine**) contains the supplementary crystallographic data for this paper. These data can be obtained free of charge from The Cambridge Crystallographic Data Centre.

3.2 Synthesis of compounds:

Synthesis of compound 1a

Obtained from 2-pyridinecarboxaldehyde (200 μ L, 2.102mmol) and 2-amino-2-methyl-1,3-propanediol (110 mg, 1.05 mmol). 89 % yield of white solid. **M.F.:** C₁₆H₁₇N₃O₂. **M.W.:** 283.33 g/mol. **d.r.**(*cis* : *trans* / 3 : 97). **M. P.:** 103-106. **IR (ATR) ν :** 2873 (*w*), 1585 (*m*), 1377 (*m*), 994 (*m*), 788 (*m*), 775 (*m*), 759 (*m*). **¹H NMR** (500 MHz, DMSO-d₆) δ = 8.19 (*m*, 2 H, H-7 and H-15), 7.51 (*m*, 4 H, H-9, H-10, H-12 and H-13), 6.98 (*m*, 2 H, H-8 and H-14), 5.61 (*s*, 1 H, H-4), 5.21 (*s*, 1 H, H-5), 4.06 (*d*, *J* = 8.5 Hz, 1 H, H-2B), 3.90 (*AB*, *J* = 22 Hz, 2 H, H-3), 3.62 (*d*, *J* = 8.5 Hz, 1 H, H-2A), 1.42 (*s*, 3 H, H-16). **¹³C NMR** (125 MHz, DMSO-d₆) δ = 159.2 (C-6), 154.5 (C-11), 148.91 (C-15), 148.4 (C-7), 136.4 (C-13), 136.1 (C-9), 123.2 (C-14), 122.7 (C-8), 122.0 (C-12), 121.8 (C-10), 93.9 (C-4), 93.6 (C-5), 77.5 (C-3), 76.0 (C-2), 70.5 (C-1), 23.5 (C-16). NMR signals corresponds to major isomer. **MS-EI+** (%) *m/z*: 283(5), 205 (21), 176 (60), 148 (75), 78 (100).

Synthesis of compound 1b

Obtained from 2-pyridinecarboxaldehyde (200 μ L, 2.102mmol) and 2-amino-1,3-propanediol (95 mg, 1.05 mmol). 85 % yield of yellow oil. **M.F:** C₁₅H₁₅N₃O₂. **M.W.:** 269.30 g/mol. **d.r.**(*cis* : *trans* / 85 : 15). **IR (ATR) ν :** 2870 (*w*), 1587 (*m*), 1377 (*m*), 994 (*m*), 788 (*m*), 780 (*m*). **¹H NMR** (200 MHz, CDCl₃) δ : 8.30 (*m*, H-7 and H-15), 7.50 (*m*, H-8, H-9, H-10, H-12, H-13 and H-14), 5.62 (*s*, H-4), 5.34 (*s*, H-5), 4.0 (*m*, H-2 and H-3). NMR signals corresponds to major isomer. **MS-EI+** (%) *m/z*: 270 (6), 191 (38), 162 (100), 131 (60), 108 (32), 78 (28).

Synthesis of compound 1c

Obtained from 4-pyridinecarboxaldehyde (200 μ L, 2.102mmol) and 2-amino-2-methyl-1,3-propanediol (110 mg, 1.05 mmol). 90 % yield of white crystals. **M.F.:** C₁₆H₁₇N₃O₂. **M.W.:** 283 g/mol. **d.r.**(*cis* : *trans*/ 6 : 94). **M. P.:** 105 °C. **IR (ATR) ν :** 2980 (w), 1630 (m), 1560 (w), 1414 (s), 1348 (s), 1237 (m). **¹H NMR** (200 MHz, CDCl₃) δ : 8.53 (*t*, 6 Hz, H-8 and H-11), 7.34 (*m*, H-7 and H-10), 5.38 (*s*, H-4 and H-5), 3.63 (*m*, H-2 and H-3), 1.18 (*s*, H-12). δ : 8.43 (*t*, 6 Hz, 4 H, H-8 and H-11), 7.23 (*d*, 6Hz, 2 H, H-7), 7.07 (*d*, 2 H, 6 Hz, H-10), 5.52 (*s*, 1 H, H-4),), 5.05 (*s*, 1 H, H-5), 3.87 (*m*, 4 H, H-2 and H-3), 1.37 (*s*, 3 H, H-12). NMR signals corresponds to major isomer. **MS-EI+** (%) *m/z*: 283 (8), 268 (20), 253 (23), 205 (80), 145 (95), 105 (73).

Synthesis of compound 1d

Obtained from 3-pyridinecarboxaldehyde (200 μ L, 2.102mmol), 2-amino-2-methyl-1,3-propanediol (110 mg, 1.05 mmol), phenyl boronic acid (128mg, 1.05mmol) 90 % yield of yellow oil. **IR (ATR) ν :** 2969 (w), 2868 (w), 1704 (w), 1643 (w), 1599 (w), 1464 (w), 1440 (*m*), 1377 (*m*), 1313 (*s*). **MS-EI+** (%) *m/z*: 283(6), 203 (75), 176 (83), 105 (80), 78 (24).

Synthesis of compound 2a-imine

Obtained from 2-pyridinecarboxaldehyde (67 μ L, 6.67 mmol), 2-amino-2-methyl-1,3-propanediol (70 mg, 6.67 mmol) and ZnCl₂ (100 mg, 667 μ mol). 87 % of white solid. **M.F.:** C₁₀H₁₄N₂O₂Zn. **M.W.:** 330.54 g/mol. **M. P.:** 184-190 °C. **IR (ATR) ν :** 3416 (-OH, *w*), 1660 (C=N, *m*), 1599 (*m*), 1443 (*m*), 1299 (*m*), 1059 (*s*), 1033 (*s*), 1014 (*s*), 928 (*m*), 772 (*s*). **¹H NMR** (500 MHz, DMSO-d₆) δ = 8.83 (*s*, 1 H, H-6), 8.61 (*broad*, 1 H, H-1), 8.25 (*t*, *J* = 7 Hz, 1 H, H-3), 8.10 (*d*, *J* = 10 Hz, 1 H, H-4), 7.83 (*t*, *J* = 5 Hz, 1 H, H-2), 6.18 (*broad*, -OH), 3.59 (*d*, *J* = 10 Hz, 2 H, H-10), 3.48 (*d*, *J* = 10 Hz, 2 H, H-8), 1.26 (*s*, 3 H, H-9).). **¹³C NMR** (125 MHz, DMSO-d₆) δ = 160.1 (C-6), 148.7 (C-1, C-5), 140.7 (C-3), 128.7 (C-2), 127.3 (C-4), 72.8 (C-7), 64.2 (C-8), 63.8 (C-9).

Synthesis of compound 2b-imine/2b-bisoxazolidine

Obtained from 2-pyridinecarboxaldehyde (67 μ L, 6.67 mmol), 2-amino-1,3-propanediol (67 mg, 667 μ mol) y ZnCl_2 (100 mg, 667 μ mol). 45 % of white solid. **M.F.:** $\text{C}_9\text{H}_{12}\text{N}_2\text{O}_2\text{Cl}_2\text{Zn}$. **M. W.:** 316.52 g/mol. **M. P. :** 194-198 $^\circ\text{C}$. **IR (ATR) ν :** 3312 (OH, *m*), 1642 (C=N, *m*), 1598 (*m*), 1441 (*m*), 1303 (*m*), 1027 (*s*), 1016 (*s*), 767 (*s*). **^1H NMR** (200 MHz, DMSO-d_6) **2b-imine** δ = 8.93 (*d*, J = 6 Hz, H-1), 8.23 (*t*, J = 6 Hz, H-3), 8.03 (*m*, H-5 and H-2), 7.81 (*m*, H-4), 5.15 (*broad*, H-9), 4.06 (*m*, H-6), 3.56 (*m*, H-7 and H-8). **2b-bisoxazolidine** δ = 8.65 (*d*, J = 6 Hz, H-1*), 8.50 (*d*, J = 6 Hz, H-4*), 7.81 (*m*, H-2*), 7.64 (*m*, H-3*), 6.35 (*s*, H-5*), 4.06 (*m*, H-7*), 3.56 (*m*, H-6*).

4. Conclusions

The direct condensation reaction of aldehydes and aminioliols predominantly yields bisoxazolidine- like compounds, as evidenced by characteristic signals around δ = 5 ppm for N-CH-O hydrogen atoms in ^1H NMR spectroscopy analysis. In addition, the X-ray diffraction analysis of compound **1d** corroborates the proposed structure for this class of compounds. The stereochemistry of the product is significantly influenced by the substituent present at the carbon atom base of the amino group (H or CH_3). The hindrance effect is minimized when only the hydrogen atom is present, leading to the formation of the *cis*-isomer as the major product. Conversely, the presence of a methyl group favors the *trans*-isomer. The theoretical calculations align with the experimental data findings, indicating that the *cis* isomer is more favorable for the hydrogen derivative, while the presence of the methyl group promotes the *trans* isomer.

Moreover, when zinc(II) serves as a template for the condensation reaction, two different metal complexes emerge as main products: imine-Zn and bisoxazolidine-Zn complexes. The substituent also plays a crucial role in determining the products distribution. In the presence of a methyl group, the imine-Zn complex is favored. However, when the substituent is only the hydrogen atom, a nearly equal mixture of imine/bisoxazolidine-Zn complexes is obtained. The formation of **2a-bisoxazolidine** hampered due to steric hindrance, particularly in achieving the *cis*-isomer. The difference in free energy between the bisoxazolidine and imine-Zn complexes indicates a clear preference for the latter ($\Delta G = 4.25 \text{ kcal mol}^{-1}$).

Acknowledgements

The authors thank Consejo Nacional de Humanidades, Ciencias y Tecnologías (CONAHCYT) for financial support through project No. 33602 and the National Laboratory of Macromolecules (LANEM) by the analytical support.

Appendix A. Supplementary data

Supplementary material related to this article can be found in the online version at:

References

1. J. M. Vega-Perez, M. Vega, E. Blanco, F. Iglesias-Guerra, *Tetrahedron Asymmetry*, **2001**, 12, 3189-3203.
2. C. Agami, F. Couty, *Eur. J. Org. Chem.*, **2004**, 4, 677-685.
3. G. H. Morales-Monarca, D. Gnecco, *Eur. J. Org. Chem.*, **2022**, 33, 70-101.
4. A. L. Braga, C. C. Silveira, M. W. G. de Bolster, H. S. Schrekker, L. A. Wessjohann, P. H. Scheneider, *J. Mol. Catal. A: Chem.*, **2005**, 239, 235-238.
5. C. A. Caputo, N. D. Jones, *Dalton Trans.*, **2007**, 4627-4640
6. C. Wolf, H. Xu, *Chem. Commun.*, **2011**, 47, 3339-3350
7. T. Arai, Y. Oginino, T. Sato, *Chem. Commun.*, **2013**, 49, 7776-7778.
8. J. D. Scott, R. M. Williams, *Chem. Rev.*, **2002**, 102, 1669-1730.
9. K. Ii, S. Ichikawa, B. Al-Dabbagh, A. Bouhss, A. Matsuda, *J. Med. Chem.*, **2010**, 53, 3793-3813.
10. J. V. Paukstelis, L. L. Lambing, *Tetrahedron Lett.*, **1970**, 4, 299-302.
11. F. Fülöp, K. Pihlaja, K. Neuvonen, G. Bernáth, G. Argay, A. Kálmán, *J. Org. Chem.*, **1993**, 58, 1967-1969.
12. K. Pihlaja, M. Juhász, H. Kivelä, F. Hülöp, *Rapid Commun. Mass Spectrom.*, **2008**, 22, 1510-1518.
13. M. Ávalos, R. Babiano, P. Cinta, J. L. Jiménez, M. E. Light, J. C. Palacios, E. M. S: Pérez, *J. Org. Chem.*, **2008**, 73, 661-672.
14. D. Talancón, R. Bosque, C. López, *J. Org. Chem.*, **2010**, 75, 3294-3300.
15. M. Juhász, L. Lázár, F. Hülöp, *Tetrahedron: Asymmetry*, **2011**, 22, 2012-2017
16. M. Hakimi, Z. Mardani, K. Moeini, M. Minoura, H. Raissi; *Z. Naturforsch.*, **2011**, 66b, 1122-1126.
17. E. S. Areas, H. C. S. Junior, B. P. Freitas, G. B. Ferreira, G. P. Guedes, *Inorg. Chim. Acta*, **2022**, 529, 120664.
18. S. L. Wiskur, M. S. Maynor, M. D. Smith, C. I. Sheppard, R. K. Akhiani, P. J. Pellechia, S. A. Vaughn, C. Shieh, *J. Coord. Chem.*, **2013**, 66, 1166-1177.
19. H. Molaei, M. Moghadam, V. Mirkhani, S. Tangestaninejad, I. Mohammadpoor-Baltork, A. A. Kajani, R. Kia, *Polyhedron*, **2019**, 160, 130-138.

20. J. Mayans, D. Gomez, M. Font-Bardia, A. Escuer, *Cryst. Growth Des.*, **2020**, 20, 6, 4176-4138.
21. C. M. Canabarro, J. Ceolin, J. D. Siquiera, B. A. Iglesias, G. M. Oliveira, D. F. Back, P. T. Campos, *J. Inorg. Gen. Chem.*, **2016**, 642, 1192-1197.
22. I. A. Gass, C. J. Gartshore, D. W. Lupton, B. Moubaraki, A. Nafady, A. M. Bond, J. F. Boas, J. D. Cashion, C. Milsman, K. Wiegardt, K. S. Murray, *Inorg. Chem.*, **2011**, 50, 3052-3064.
23. J. Ceolin, J. D. Siqueira, F. M. Martins, P. C. Piquini, B. A. Iglesias, D. F. Back, G. M. Oliveira, *Appl. Organomet. Chem.*, **2018**, e4218, 1-15.
24. I. A. Gass, M. Asadi, D. W. Lupton, B. Moubaraki, A. M. Bond, S. Guo, K. S. Murray, *Aust. J. Chem.*, **2014**, 67, 1618-1624.
25. Z. Mardani, *J. Struct. Chem.*, **2020**, 62, 6, 852-860.
26. A. Saleem, P. A. Kobielska, K. Harms, M. G. Katsikogianni, R. Terlford, G. Novitch, S. Nayak, *Dalton Trans.*, **2018**, 47, 6156-6165.
27. Z. Mardani, V. Golsanamlou, S. Khodavandegar, K. Moeini, A. M. Z. Slain, J. D. Woollins, *J. Coord. Chem.*, **2018**, 71, 120-134.
28. Z. Mardani, M. Hakimi, K. Moenin, F. Mohr, *Acta Cryst. C*, **2019**, C75, 1-9.
29. M. Darabantu, C. Maieranu, I. Silagui, -Dumitrescu, L. Toupet, E. Condamine, Y. Ramondenc, C. Berghian, G. Plé, N. Plé, *Eur. J. Org. Chem.*, **2004**, 2644-2661.
30. O. Nachtigall, A. I. VanderWeide, W. W. Brennessel, W. D. Jones, *J. Inorg. Gen. Chem.*, **2021**, 647, 1-8.
31. O. Nachtigall, A. I. VanderWeide, W. W. Brennessel, W. D. Jones, *ACS Catal*, **2021**, 11, 10885-10891.
32. S. Karim, A. Chakraborty, D. Samantha, E. Zangrando, T. Ghosh, D. Das, *Catal. Sci. Technol.*, **2020**, 10, 2830-2837.
33. M. Darabantu, G. Plé, C. Maieranu, I. Silaghi-Dumitrescu, Y. Ramondenc, S. Mager, *Tetrahedron*, **2000**, 56, 3799-3816.
34. S. Monge, J. Sélambarom, F. Carré, J. Verducci, J. Roque, A. A. Pavia, *Carbohydr. Res.*, **2000**, 328, 127-133.
35. H. López-Ruiz, H. Briño-Ortega, S. Rojas-Lima, R. Santillan, N. Farfán, *Tetrahedron Lett.*, **2011**, 52, 4308-4312.

36. A. Visnjevac, L. Tusek-Bozic, M. Majeric-Elenkov, Z. Hamersak, H. Kooijma, E. D. Clercq, B. Kojic-Prodic, *Polyhedron*, **2002**, 21, 2567-2577.
37. M. Schulz, M. Klopfleisch, H. Görls, M. Kahnes, M. Westerhausen, *Inorg. Chim. Acta*, **2009**, 362, 4706-4712.
38. A. Erxleben, *Inorg. Chem.*, **2001**, 40, 208-213.
39. X. Sun, C. Qi, S. Ma, H. Huang, W. Zhu, Y. Liu, *Inorg. Chem. Commun.*, **2006**, 9, 911-914.
40. A. W. Addison, T. N. Rao, J. Reedijk, J. V. Rijn, G. C. Verschoor, *Dalton Trans.*, **1984**, 1349-1356.
41. J. Wirbser, H. Vahrenkamp, *Z. für Naturforsch. - B J. Chem. Sci.*, **1992**, 47, 962-968.
42. D. M. J. Frisch, G. W. Trucks, H. B. Schlegel, G. E. Scuseria, M. A. Robb, J. R. Cheeseman, G. Scalmani, V. Barone, B. Mennucci, G. A. Petersson, H. Nakatsuji, M. Caricato, X. Li, H. P. Hratchian, A. F. Izmaylov, J. Bloino, G. Zheng, J. L. Sonnenberg, M. Hada, M. Ehara, K. Toyota, R. Fukuda, J. Hasegawa, M. Ishida, T. Nakajima, Y. Honda, O. Kitao, H. Nakai, T. Vreven, J. A. Montgomery Jr, J. E. Peralta, F. Ogliaro, M. Bearpark, J. J. Heyd, E. Brothers, K. N. Kudin, V. N. Staroverov, R. Kobayashi, J. Normand, K. Raghavachari, A. Rendell, J. C. Burant, S. S. Iyengar, J. Tomasi, M. Cossi, N. Rega, J. M. Millam, M. Klene, J. E. Knox, J. B. Cross, V. Bakken, C. Adamo, J. Jaramillo, R. Gomperts, R. E. Stratmann, O. Yazyev, A. J. Austin, R. Cammi, C. Pomelli, J. W. Ochterski, R. L. Martin, K. Morokuma, V. G. Zakrzewski, G. A. Voth, P. Salvador, J. J. Dannenberg, S. Dapprich, A. D. Daniels, O. Farkas, J. B. Foresman, J. V. Ortiz, J. Cioslowski, D. J. Fox, C. T. Wallingford, Gaussian, Inc, **2009**.
43. A. D. Becke, *J. Phys. Chem.*, **1993**, 98, 5648-5652.
44. P. J. Stephens, F. J. Devlin, C. F. Chabalowski, M. J. Frisch, *J. Phys. Chem.*, **1994**, 98, 11623-11627.
45. W. J. Hehre, R. Ditchfield, J. A. Pople, *J. Phys. Chem.* **1972**, 56, 2257-2261.
46. CrysAlisPro, Oxford Diffraction, Agilent Technologies UK Ltd, Yarnton, England, **2014**.
47. O. V. Dolomanov, L. J. Bourhis, R. J. Gildea, J. A. K. Howard, H. Puschmann, *OLEX2, J. Appl. Crystallogr.*, **2009**, 42, 339-341.
48. G. M. Sheldrick, *Acta Crystallogr. C Struct. Chem.* **2015**, 71, 3-8.

49. C. F. Macrae, P. R. Edgington, P. McCabe, E. Pidcock, G. P. Shields, R. Taylor, M. Towler, J. van de Streek, *J. Appl. Crystallogr.*, **2006**, 39, 453-457.
50. H. Putz, K. Brandeburg, *Crystal Impact*. 102, 53227 Bonn, Germany.